Carbohydrate Polymers 114 (2014) 321–329

Contents lists available at ScienceDirect

Carbohydrate Polymers

journal homepage: www.elsevier.com/locate/carbpol

Synthesis and flocculation properties of gum ghatti and poly(acrylamide-co-acrylonitrile) based biodegradable hydrogels

Hemant Mittal[a,c,*], Rajeev Jindal[b], Balbir Singh Kaith[b], Arjun Maity[c], Suprakas Sinha Ray[a,c,*]

[a] Department of Applied Chemistry, University of Johannesburg, Doornfontein 2028, South Africa
[b] Department of Chemistry, National Institute of Technology, Jalandhar 144011, Punjab, India
[c] DST/CSIR National Centre for Nanostructured Materials, Council for Scientific and Industrial Research, Pretoria 0001, South Africa

ARTICLE INFO

Article history:
Received 13 June 2014
Received in revised form 30 July 2014
Accepted 7 August 2014
Available online 23 August 2014

Keywords:
Gum ghatti
Hydrogel
Swelling
Flocculation
Biodegradation
Adsorption

ABSTRACT

This article reports the development of biodegradable flocculants based on graft co-polymers of gum ghatti (Gg) and a mixture of acrylamide and acrylonitrile co-monomers (AAm-co-AN). The hydrogel polymer exhibited an excellent swelling capacity of 921% in neutral medium at 60 °C. The polymer was used to remove saline water from various petroleum fraction-saline water emulsions. The flocculation characteristics of the hydrogel polymer were studied in turbid kaolin solution as a function of the amount of polymer and the solution temperature and pH. Biodegradation studies of hydrogel polymer were conducted using the soil composting method, and the degradation process was constantly monitored using scanning electron microscopy and Fourier transform infrared spectroscopy techniques. The results demonstrated an 89.47% degradation of the polymer after 60 days. Finally, the hydrogel polymer adsorbed 98% of cationic dyes from the aqueous solutions.

1. Introduction

In recent decades, synthetic polymers have been extensively used by many industries because of their excellent mechanical and physical properties. However, the main disadvantage of synthetic polymers is their non-degradable nature, which makes their disposal difficult. Recently, researchers have made a variety of attempts to replace non-degradable polymers with biodegradable polymers (Averous & Pollet, 2013; Hermanova et al., 2013; Liang et al., 2013; Okada, 2002; Zare, Lakouraj, & Mohseni, 2014). Biodegradation is the process of the fragmentation of long polymer chains into low molecular weight compounds in the presence of microorganisms. Biodegradation of polymers depends upon several factors including the chemical and physical properties of polymers, the composition of the final product and the length and crystallinity of the polymer chains (Abrusci, Marquina, & Catalina, 2007; Nageotte, Pester, Pradet, & Bayard, 2006). The experimental conditions including temperature and humidity also influence the biodegradability of polymers.

While biopolymers are highly biodegradable, they tend to have poor properties compared to synthetic polymers. Biopolymers also have some potential advantages over synthetic polymers, including their excellent biocompatibility, their eco-friendly nature, low cost, abundant availability, and suitability for use in many biomedical applications (Jenkins, Samuel, & Hudson, 2001; Park, Park, & Kim, 2006). Moreover, the inherent properties of biopolymers can be improved through a variety of techniques including graft co-polymerization. Graft co-polymerization is the most widely studied technique to improve the inherent properties of biopolymers, and it has mainly been used for polysaccharide-based biopolymers. Recently, many studies have been carried out on the graft co-polymerization of gum polysaccharides such as gum ghatti, gum xanthan, gum arabic and guar gum (Kaith, Ranjta, & Kumar, 2008; Mittal, Fosso-Kankeu, Mishra, & Mishra, 2013; Mittal, Ballav, & Mishra, 2014; Sand, Yadav, Mishra, Tripathy, & Behari, 2011; Sanghi, Bhattacharya, & Singh, 2006), and the resulting graft co-polymers have potential applications in the food industry, as drug delivery devices, in soft tissue engineering and waste water treatment (Mariano, El Kissi, & Dufresne, 2014; Mittal & Mishra, 2014; Sand, Yadav, & Behari, 2010; Sarkar, Mandre, Panda, & Pal, 2013; Thakur, Thakur, Raghavan, & Kessler, 2014).

* Corresponding authors at: Department of Applied Chemistry, University of Johannesburg, Doornfontein 2028, South Africa. Tel.: +27 847067375; fax: +27 128412229.
E-mail addresses: mittal.hemant5@gmail.com (H. Mittal), rsuprakas@csir.co.za (S.S. Ray).

http://dx.doi.org/10.1016/j.carbpol.2014.08.029
0144-8617/

The anionic polysaccharide gum ghatti (Gg) is an exudate of the *Anogeissus latifolia* tree, which belongs to the *Combretaceae* family. The structure of Gg is composed of sugars such as L-arabinose, D-galactose, D-mannose, D-xylose and D-glucoronic acid in a 48:29:10:5:10 molar ratio (Aspinall, Hirst, & Wickstrom, 1955). The molecular structure of Gg contains alternating 4-O-substituted and 2-O-substituted α-D-mannopyranose units and chains of 1 → 6 linked β-D-galactopyranose units with side chains that are most frequently single L-arabinofuranose residues (Aspinall, 1980; Mittal, Mishra, Mishra, Kaith, & Jindal, 2013) (Fig. S1, supplementary data).

The process of removing different organic and inorganic impurities from waste water by converting suspended particles into heavy flocs is called flocculation. Flocculation is a highly efficient technique for the purification of industrial and domestic wastewater and the thickening of sludge. Flocculants can be either inorganic, usually called coagulant agents (such as aluminum sulfate and ferric chloride), or polymeric materials (Ghimici, Constantin, & Fundueanu, 2010). The properties of polymer-based flocculants can be easily tailored to specific applications. Moreover, the flocculation capacity of polymer-based flocculants is much higher than that of inorganic flocculants (Singh et al., 2000). Polymer-based flocculants can be synthetic (Ghimici, Dranca, Dragan, Lupascu, & Maftuleac, 2001; Nasser & James, 2006) or natural (Ghimici & Constantin, 2011; Pal, Sen, Karmakar, Mal, & Singh, 2008; Simon, Picton, Le Cerf, & Muller, 2005). Synthetic polymer-based flocculants exhibit better performance than natural polymer-based flocculants. However, natural polymer-based flocculants have their own advantages including low cost, biodegradability and non-toxicity (Ghimici et al., 2010). Therefore, it is critical to develop flocculant materials with the advantages of both synthetic and natural polymers. Recently, a great deal of work has been reported aiming to develop flocculants through the graft co-polymerization of polysaccharides with synthetic vinyl monomers, such as poly(acrylic acid) and poly(acrylamide) (Chang, Hao, & Duan, 2008; Mittal, Mishra, et al., 2013; Singh et al., 2000; Tian & Xie, 2008; Wan, Li, Wang, Chen, & Gu, 2007).

The purification of industrial effluent water is one of the greatest challenges faced by developing countries. Industries producing batteries, textiles, paper, cosmetics and ink generate huge amounts of wastewater contaminated with various types of dyes. It is very difficult to degrade dyes in sludge treatment plants because most dyes are non-degradable in nature (Kumari & Abraham, 2007). Adsorption is one of the most efficient techniques used for the treatment of dye-contaminated water. In this direction, gum polysaccharide-based graft co-polymers have demonstrated their potential to efficiently adsorb dyes from wastewater (Ghorai, Sarkar, Raoufi, Panda, & Schonherr, 2014; Mittal & Mishra, 2014; Mittal et al., 2014).

While researchers have tested these polymers for their flocculation characteristics, swelling properties and ability to adsorb pollutants from contaminated water, these polymers do not exhibit these key properties, resulting in poor performance. Furthermore, synthesized graft co-polymers exhibited considerable resistance to biodegradation (Mishra, Sand, Mishra, Yadav, & Behari, 2010; Sand et al., 2010, 2011). In previous studies, we also reported the swelling properties, flocculation characteristics and biodegradation of cross-linked graft co-polymers of Gg with AAm (Mittal, Mishra, et al., 2013) and with the co-polymer mixture of AAm with the hydrophilic vinyl monomer acrylic acid (AA) (Mittal, Mishra, et al., 2013). The current study reports the effect of a co-polymer mixture of AAm with a hydrophobic vinyl monomer, i.e., acrylonitrile (AN) on the flocculation characteristics, swelling properties, thermal stability, adsorption efficiency and biodegradation behavior of a cross-linked graft co-polymer of Gg.

2. Experimental

2.1. Materials

AAm, AN, Gg, N,N′-methylene-bis-acrylamide (MBA), potassium persulfate (KPS), ascorbic acid (ABC), petroleum ether, methylene blue, rhodamine B and kaolin were purchased from Merck Chemicals (India) and used as received. Petrol and diesel were purchased from Indian Oil Corporation Limited, India. All chemicals were of analytical grade and were used as received without further purification. All solutions were prepared in triple-distilled water. Flocculation studies were conducted on a Micro 1000 IR Turbidimeter (HF Scientific Incorporation, USA). Stock solutions of dyes (1000 mg l^{-1}) were prepared by dissolving the appropriate amount of dye in sterile distilled water; adequate volumes of the stock solutions were further diluted in distilled water to prepare experimental solutions.

2.2. Synthesis of the Gg-cl-P(AAm-co-AN) hydrogel polymer

The cross-linked hydrogel polymer of Gg with the co-polymer mixture of P(AAm-co-AN) was prepared using graft co-polymerization (Kaith, Jindal, & Mittal, 2010). At first, 1 g of Gg was added to 30 ml distilled water and left undisturbed for 24 h to obtain a homogeneous mixture of gum polysaccharide in water. After 24 h, a mixture of KPS (30 mg) and ABC (20 mg) was added to the reaction mixture with constant stirring, followed by the addition of MBA (50 mg). The reaction temperature was maintained at 60 °C. The monomer mixture of AAm (1.0 g) and AN (2.0 ml) was added to the reaction vessel. The reaction was allowed to continue for the next 6 h. After that, the reaction vessel was removed and cooled to room temperature. The homopolymers polyacrylamide and polyacrylonitrile and the unreacted co-polymer P(AAm-co-AN) were removed by successive extractions with acetone and N,N′-dimethylformamide, respectively. Finally, the synthesized hydrogel was dried in a hot air oven at 60 °C until a constant weight was achieved.

2.2.1. Characterization

Changes in the thermal behavior of Gg after graft co-polymerization and cross-linking with P(AAm-co-AN) and MBA were studied using TGA/DTA/DTG (TG/DTA 6300, SII EXSTAR 6000, SII Nanotechnology Incorporation, Japan) in air at a heating rate of 10 °C per minute. The FTIR spectra of the Gg and the Gg-cl-P(AAm-co-AN) hydrogel polymer before degradation and at various stages of degradation were recorded on a PERKIN ELMER RXI spectrophotometer using KBr pellets (Sigma–Aldrich) in the spectral range of 4000–400 cm^{-1} with a resolution of 4 cm^{-1}. The morphological change of the hydrogel polymers at various stages of biodegradation was examined using SEM (LEO, 435 VF, LEO Electron Microscopy Ltd., Japan). As all samples were non-conductive, they were coated with gold to introduce conductivity.

2.3. Swelling studies in deionized water

As the ability to swell in water is one of the most important features of hydrogels, it is very important to determine the swelling capacity of the synthesized hydrogel polymer. The swelling efficiency of the Gg-cl-P(AAm-AN) hydrogel polymer was investigated at various time intervals (4, 8, 12, 16, 20 and 24 h), temperatures (30, 40, 50, 60 and 70 °C) and pH values (3.0–13.0) in deionized water. For each experiment, several 100 mg of samples of hydrogel polymer were each immersed in 100 ml of deionized water. After a particular time interval, the samples were removed, gently wiped

and weighed. The percentage swelling (P_s) was then calculated using Eq. (1) (Kaith, Jindal, Mittal, & Kumar, 2012):

$$P_s = \frac{W_s - W_d}{W_d} \times 100 \quad (1)$$

where W_s and W_d are the weights of the swelled and dry hydrogel polymer samples, respectively.

After the swelling time was optimized, the effect of temperature on P_s was studied at a pre-optimized time, and then the pH of the swelling medium was optimized to obtain the maximum P_s at the pre-optimized time and temperature.

2.3.1. Selective absorption of saline from various petroleum fraction-saline emulsions

The separation of saline water from crude petroleum during their extraction from the sea is challenging because current processes are highly tedious and expensive. The hydrogel polymers synthesized here were tested for the selective absorption of saline water from various petroleum fraction-saline emulsions. A 1% NaCl solution was used as saline water with various petroleum fractions such as kerosene, diesel, petrol and petroleum ether. From each emulsion, 50 ml (i.e., 25 ml of saline water and 25 ml of the petroleum fraction) was collected in a 250 ml conical flask. A stable emulsion was prepared by adding 10 ml tween-20, and the flasks were shaken using an automatic shaker machine (LABCO, India). Once a stable emulsion was obtained, 100 mg of hydrogel polymer was added. After 16 h, the flasks were removed from the shaker and allowed to stand undisturbed for 48 h to break up the emulsions. The petroleum fractions were then separated using a separating funnel, and the remaining unabsorbed volume of saline water was measured.

2.4. Flocculation studies

Flocculation characteristics of the Gg-cl-P(AAm-AN) hydrogel polymer were investigated using the standard jar test (Jha, Agarwal, Mishra, & Rai, 2001; Mittal, Mishra, et al., 2013). For each experiment, a volume of 500 ml of the 50 ppm kaolin solution was placed in 1000 ml and agitated at 180 rpm for 10 min. Initially, a blank reading was taken followed by the addition of hydrogel polymer to the kaolin suspension. Readings were taken every 10 min until almost constant turbidity was obtained. Different doses of the hydrogel polymer were used to determine the optimal dose to maximize flocculation capacity. The flocculation temperature was then optimized, followed by the solution pH.

2.5. Biodegradation studies

The biodegradation of the Gg-cl-P(AAm-AN) hydrogel polymer was studied using the soil composting method (Kaith, Jindal, Maiti, & Jana, 2010). Biodegradation studies were performed in flower pots, and the compost was collected from the waste water effluent discharge plant of the National Institute of Technology, Jalandhar, India (Fig. 1). For each experiment, rectangular samples (2 cm × 2 cm × 1.5 cm) were prepared and buried in soil compost in a flower pot at a depth of 2 cm, 3 cm apart from each other. Microbe rich water from the plant was added to the compost on alternating days to compensate for water loss caused by evaporation. The progress of the degradation process was examined every 5 days. Every 5 days, the samples were extracted from the compost, carefully cleaned, dried at 50 °C in a vacuum oven and weighed.

The percentage weight loss at each stage of degradation was calculated using Eq. (2) (Kaur, Bhalla, Deepika, & Gautam, 2009):

$$\text{Weight loss}(\%) = \frac{w_i - w_t}{w_i} \times 100 \quad (2)$$

where W_i is the initial weight of the hydrogel polymer and W_t is the weight after a particular time interval.

The progress of degradation was also evaluated by studying the changes in physical appearance and chemical composition using SEM and FTIR, respectively.

2.6. Adsorption of methylene blue and rhodamine B from the aqueous solution

Adsorption studies of the cationic dyes methylene blue and rhodamine B were carried out in batch mode. A 50 mg l^{-1} solution of each dye (50 ml) was first placed in 100 ml glass bottles. Various amounts of the Gg-cl-P(AAm-co-AN) hydrogel polymer were added to each dye solution. The bottles were placed in a thermostatic water bath and shaken for 24 h at 200 rpm. After 24 h, the bottles were removed from the water bath and the dye solutions were filtered using a 0.45 μm cellulose acetate syringe filter. The concentration of unadsorbed dye remaining in the solution was analyzed using a UV/vis spectrophotometer (Shimadzu, Japan UV-2450, UV–vis spectrophotometer) at 554 nm as the λ_{max} of rhodamine B and 664 nm as the λ_{max} of methylene blue. The adsorption efficiency or the percentage removal was calculated using Eq. (3) (Sadeghi, Azhdari, Arabi, & Moghaddam, 2012):

$$\%\text{removal} = \frac{(C_o - C_e)}{C_o} \times 100 \quad (3)$$

3. Results and discussion

3.1. Thermogravimetric analysis, differential thermal analysis and differential thermo-gravimetric analysis (TGA/DTA/DTG)

The initial decomposition temperature (IDT) of the Gg-cl-P(AAm-co-AN) hydrogel polymer was found to be 133.6 °C (Fig. S2, supplementary data), which was much lower than the IDT of the Gg, i.e., 206.9 °C (Mittal, Mishra, et al., 2013). In contrast, the final decomposition temperature (FDT) of the Gg-cl-P(AAm-co-AN) hydrogel polymer (681.8 °C) was found to be much higher than the FDT of the Gg (521.6 °C) (Mittal, Mishra, et al., 2013). The graft co-polymerization of the Gg with the binary monomer mixture of P(AAm-co-AN) decreases the IDT. This may be associated with the degradation of P(AAm-co-AN) chains as a result of the formation of the imide group with the evolution of ammonia. Furthermore, as the formation of amide groups increased the FDT of the graft co-polymer, a higher FDT was observed in the case of the Gg-cl-P(AAm-co-AN) hydrogel polymer compared to Gg (Behari, Pandey, Kumar, & Taunk, 2001). The Gg-cl-P(AAm-co-AN) hydrogel polymer degradation curve also exhibited three stages of decomposition ranging from 133.6 to 276.8 °C (weight loss, 17.3%), 276.8 to 436.2 °C (weight loss, 18.3%) and 436.2 to 681.1 °C (weight loss, 61.3%). In contrast, the TGA of the Gg exhibited two stage decomposition over the temperature ranges from 206.9 to 331.4 °C (weight loss, 46.6%) and 331.4 to 521.6 °C (weight loss, 31.2%). Moreover, a detailed study of the percentage weight loss at different temperatures indicated that in Gg, a certain percentage weight loss occurred at lower temperatures compared to the Gg-cl-P(AAm-co-AN) hydrogel polymer (Table S1, supplementary data).

The DTA of the Gg exhibited two exothermic peaks at 483.2 °C (203 μV) and 492.7 °C (154 μV), whereas the DTA of the Gg-cl-P(AAm-co-AN) hydrogel polymer exhibited exothermic peaks at 280.8 °C (102.2 μV) and 669.9 °C (136.2 μV). DTA peaks were observed at much higher temperatures with less heat evolved in the DTA of the Gg-cl-P(AAm-co-AN) (Fig. S2, supplementary data) compared to the Gg (Mittal, Mishra, et al., 2013). The Gg-cl-P(AAm-co-AN) hydrogel polymer exhibited two DTG peaks at 280.8 °C with

Fig. 1. (a and b) Images of the sludge treatment plant at the NIT, Jalandhar, India and (c) an image of a flower pot containing soil compost for biodegradation studies.

a mass loss rate of 2.223 mg/min and at 669.4 °C with a mass loss rate of 1.01 mg/min (Fig. S2, supplementary data). In contrast, the DTG of the Gg exhibited decompositions at 299.1 °C and 479.0 °C with mass loss rates of 1.463 and 2.23 mg/min, respectively (Mittal, Mishra, et al., 2013). DTG studies showed that the rate of thermal decomposition was higher in Gg than in the Gg-cl-P(AAm-co-AN) hydrogel polymer. Thus, TGA/DTA/DTG studies suggest that the thermal stability of Gg improved after including P(AAm-co-AN) chains in the backbone polymer through graft co-polymerization and cross-linking.

3.2. Swelling studies of the Gg-cl-P(AAm-co-AN) hydrogel polymer in deionized water

3.2.1. Effect of time on P_s

The effect of swelling time on P_s was studied at various time intervals (4, 8, 12, 16, 20 and 24 h) (Fig. 2(a)). Initially, the P_s was found to increase with increasing swelling time, reaching a maximum P_s (669%) after 16 h. Further increases in swelling time did not lead to any further increases in swelling capacity, and almost a constant value of P_s was observed. This may be because after reaching maximum swelling, the three dimensional porous network of the Gg-cl-P(AAm-co-AN) hydrogel polymer becomes fully saturated, with no more active sites available to accommodate water molecules. Therefore, no increase in swelling capacity was observed after 16 h swelling time.

3.2.2. Effect of temperature on P_s

The effect of temperature on P_s was studied at various temperatures (30, 40, 50, 60 and 70 °C) at the pre-optimized swelling time (16 h) (Fig. 2(b)). Initially, swelling capacity was found to increase with increasing temperature up to 60 °C, reaching a maximum value of P_s (921%). However, with further increases in temperature, the P_s of the Gg-cl-P(AAm-co-AN) hydrogel polymer decreased remarkably, reaching 863% at 70 °C. This suggests that increases in temperature initially increased the elasticity of the cross-linked hydrogel polymer network, resulting in a larger P_s, but above the optimal temperature the polymer network collapsed, leading to desorption with further increases in temperature (Zhang, Yang, Chung, & Ma, 2001). Moreover, the hydrophilic groups of the hydrogels formed hydrogen bonds with water molecules. These bonds cooperatively formed a stable shell of hydration around the hydrophilic groups, increasing the uptake of water and thus increasing P_s. However, the associated interactions among the hydrophilic groups released the entrapped water molecules from the hydrogel network at higher temperatures. Therefore, a lower P_s value was observed at higher temperatures (Feil, Bae, Feijen, & Kim, 1992; Inomato, Goto, & Saito, 1990).

3.2.3. Effect of pH on P_s

Solution pH was found to have a profound effect on the swelling of hydrogel polymers, as reported by a number of researchers (Mahdavinia, Pourjavadi, Hosseizadeh, & Zohuriaan, 2004; Mittal, Mishra, et al., 2013). The effect of pH on the P_s of the Gg-cl-P(AAm-co-AN) hydrogel polymer was studied in solutions with pH values ranging from 3.0 to 13.0 at the pre-optimized swelling time and temperature (Fig. 2(c)). A higher value of P_s was observed in the solution at neutral pH (921%) compared to acidic and alkaline pH solutions. The swelling capacity of the hydrogel polymer increased with solution pH. This type of swelling behavior can be explained based on osmotic swelling pressure theory. In the case of dilute electrolyte solutions, the swelling capacity of the hydrogel polymers depends on osmotic swelling pressure (π_{ion}), given as (Bajpai, 1999):

$$\pi_{ion} = RT \sum (C_i^g - C_i^s) \quad (4)$$

where C_i^g and C_i^s are the molar concentrations of mobile ions in the swollen gel and external solution, respectively. R and T are the gas constant and absolute temperature, respectively.

In the solutions of neutral medium, the concentration of mobile ions (C_i^s) in swelling medium became very small, increasing the value of π_{ions}. In contrast, in acidic solutions, most of the carboxylate ions were protonated (Mahdavinia et al., 2004), decreasing the concentration of mobile ions within the swollen gel (C_i^g), leading to a reduced value of π_{ions}. Furthermore, in alkaline solutions, —COOH groups completely dissociated and Na^+ and —OH ions were present at very high concentration, reducing the values of π_{ions} and P_s (Mahdavinia et al., 2004; Mittal, Mishra, et al., 2013).

3.2.4. Selective absorption of saline from different petroleum fraction-saline emulsions

Initially, the swelling behavior of the Gg-cl-P(AAm-co-AN) hydrogel polymer was tested in different petroleum fractions, i.e., petrol, kerosene, diesel and petroleum ether, and the hydrogel polymer did not absorb any of these petroleum fractions. The maximum saline adsorption was observed in the petroleum ether-saline emulsion (25.5%) followed by the petrol-saline emulsion (23.5%), the kerosene-saline emulsion (21.0%) and the diesel-saline emulsion (18.7%) (Table 1). This adsorption trend can be attributed to the length of hydrocarbon chains present in the various petroleum fractions. Petroleum fractions with larger hydrocarbon chains have large hydration shells, impeding the absorption of water molecules by the hydrogel polymer. As petroleum ether has the fewest carbon atoms (C < 12), followed by petrol (C_4–C_8), kerosene (C_{10}–C_{15}) and diesel (C > 15), the maximum adsorption of saline was observed in the petroleum ether-saline emulsion, followed by the petrol-saline emulsion, the kerosene-saline emulsion and the diesel-saline emulsion (Mittal, Mishra, et al., 2013).

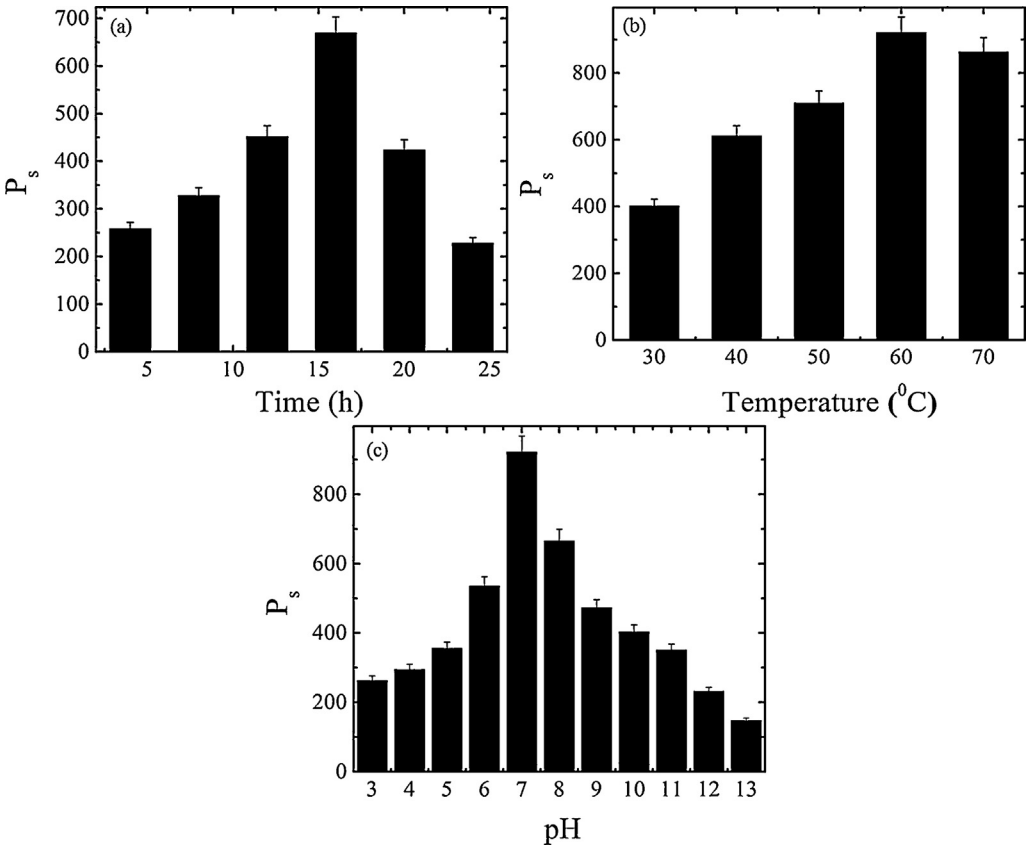

Fig. 2. Effects of (a) time, (b) temperature and (c) pH on the P_s of the Gg-cl-P(AAm-co-AN) hydrogel polymer.

3.3. Characterization of the flocculation of the Gg-cl-P(AAm-co-AN) hydrogel polymer

3.3.1. Effect of polymer dose on flocculation efficiency

The effect of the amount of the Gg-cl-P(AAm-co-AN) hydrogel polymer on the turbidity of the kaolin suspension was studied in the presence of various masses of hydrogel polymer (10, 15, 20 and 25 mg l^{-1}) in a neutral medium. Initially, the turbidity of the kaolin suspension decreased with increasing amounts of hydrogel polymer, reaching a minimum value of 2144 NTU with 15 mg l^{-1} polymer (Fig. 3(a)). However, further increases in the amount of hydrogel polymer resulted in increases in turbidity. The gradual initial decrease in the turbidity of the kaolin suspension was due to the formation of particle–polymer–particle complexes between the kaolin particles and the Gg-cl-P(AAm-co-AN) hydrogel polymer, where the hydrogel polymer acted as a bridge between different suspended kaolin particles (Mittal, Mishra, et al., 2013; Tian & Xie, 2008). Kaolin particles attached to different functional groups present on the polymer chain as soon as they came into contact with the hydrogel polymer, leading to the formation of extended polymer chains. In the presence of lower amounts of polymer, insufficient functional groups were available to act as bridges between different clay particles. However, as the polymer dose was increased the number of functionalities increased, increasing the number of bridges accessible for the formation of particle–polymer–particle complexes, decreasing the turbidity value. Therefore, increasing the amount of hydrogel polymer initially resulted in a gradual decrease in turbidity. Further increases in the amount of hydrogel polymer beyond the optimum increased the turbidity of the kaolin suspension because beyond the optimum dose, kaolin particles will envelope between different polymer chains, thus failing to come into contact with the functional groups of the hydrogel polymer (Xie, Feng, Cao, Xia, & Lu, 2007). Kaolin particles in suspension will be re-stabilized, resulting in a higher turbidity value. Therefore, particle–polymer–particle complexes will not be formed in the presence of excessive amounts of hydrogel polymer, resulting in a higher turbidity value (Ghimici & Nichifor, 2010; Ghimici & Nichifor, 2012; Ghimici, Constantin, & Fundueanu, 2012).

3.3.2. Effect of temperature on flocculation efficiency

The effect of temperature on the flocculation efficiency of the Gg-cl-P(AAm-co-AN) hydrogel polymer is shown in Fig. 3(b). Initially, turbidity was found to decrease with increasing

Table 1
Percentage removal of saline from different petroleum fraction-saline emulsions.

Sample	Percentage saline removal											
	Kerosene-saline			Diesel-saline			Petrol-saline			Pet. ether-saline		
	% Removal	±SD	±SE	% Removal	±SD	±SE	% Removal	±SD	±SE	% Removal	±SD	±SE
Gg-cl-P(AAm-co-AN)	21.0	1.27	0.73	18.7	0.51	0.30	23.5	0.52	0.30	25.5	0.87	0.50

Whereas, no. of replications = 03; amount of each emulsion taken = 100 ml (1:1, v/v); weight of superabsorbent taken for each emulsion = 1.0 g.

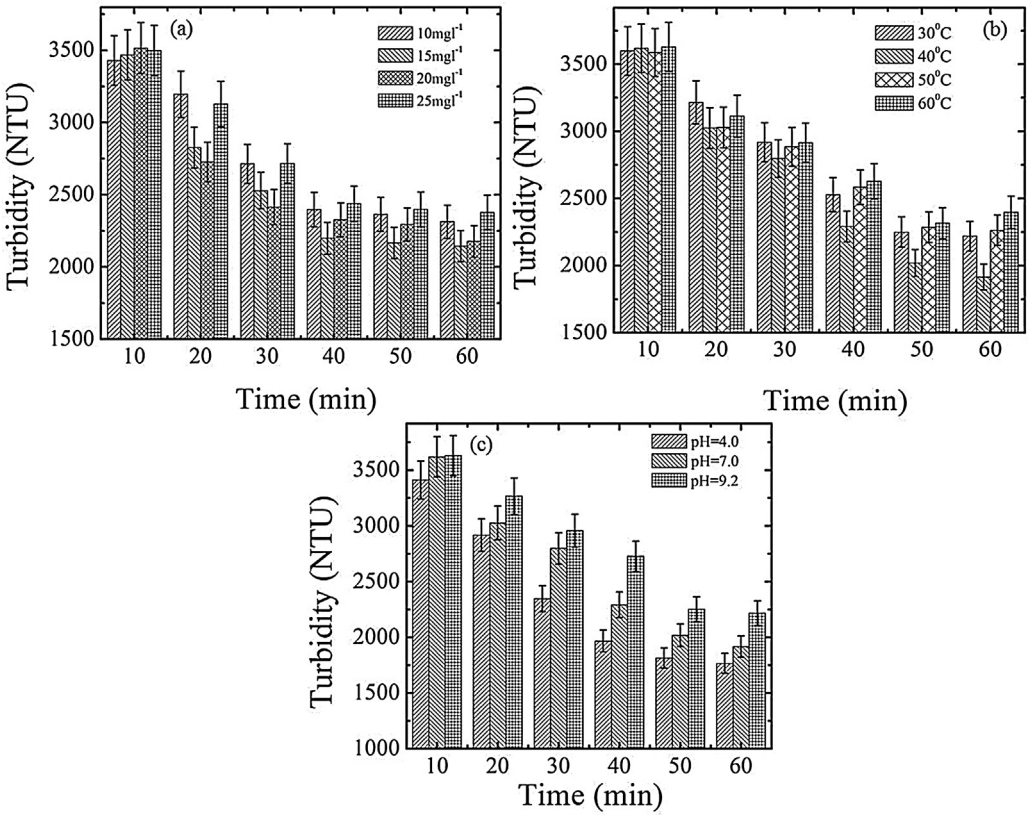

Fig. 3. Effects of (a) polymer dose, (b) temperature, (c) pH on turbidity.

temperature, reaching a minimum value of 1915 NTU at 40 °C. Further increases in temperature beyond the optimum value increased the turbidity of the kaolin solution. The initial decrease in the turbidity of the kaolin solution was associated with the formation of particle–polymer–particle complexes and was supported by the initial increase in temperature. However, at higher temperatures, the kinetic energy of hydrogel polymer molecules was increased, resulting in the re-dispersion of kaolin particles and a higher turbidity value (Mittal, Mishra, et al., 2013).

3.3.3. *Effect of pH on flocculation efficiency*

The effect of the solution pH on the flocculation efficiency of the Gg-cl-P(AAm-co-AN) hydrogel polymer was examined in kaolin solutions of various pH values at the pre-optimized polymer dose and temperature (Fig. 3(c)). The minimum turbidity of the kaolin solution was observed at acidic pH, and the turbidity of the kaolin solution increased with increasing solution pH, with the maximum turbidity observed in the kaolin solution at alkaline pH. The turbidity was lower in acidic solutions because under acidic conditions, the hydroxyl and carboxylate groups present in the Gg-cl-P(AAm-co-AN) hydrogel polymer were protonated, imparting a cationic charge to the overall hydrogel polymer network (Mittal, Mishra, et al., 2013). Negatively charged kaolin particles were easily attached to those cationic sites, forming larger flocks that easily settled, resulting in a reduction in the turbidity of the kaolin solution. In alkaline solutions, amides are weakly acidic and resonance stabilized (Mittal, Mishra, et al., 2013). Therefore, due to the anionic-anionic repulsion between the functional groups of the Gg-cl-P(AAm-co-AN) hydrogel polymer and kaolin particles, particle–polymer–particle complexes were not formed and little decrease in the turbidity of the kaolin solution was observed.

3.4. *Biodegradation studies of the Gg-cl-P(AAm-co-AN) hydrogel polymer*

While biopolymers are well-suited for many applications due their biodegradable nature, they also have serious shortcomings for many applications. Therefore, many biopolymers need to be chemically modified without affecting the biodegradable nature of the biopolymer. Here, we studied the effect of graft co-polymerization and crosslinking of Gg with the binary monomer mixture of P(AAm-co-AN) on its biodegradability. In the Gg-cl-P(AAm-co-AN) hydrogel polymer, the process of biodegradation starts with the backbone polymer, i.e., Gg. The weight of the hydrogel polymer was measured every 5 days (Table 2). The biodegradation process was found to be continuous in terms of the percentage weight loss of the Gg-cl-P(AAm-co-AN) hydrogel polymer versus time. The Gg-cl-poly(AAm-co-AA) hydrogel polymer degraded by up to 89.47% over 60 days. The polymer samples were both enzymatically and chemically degraded. Furthermore, the secretion products of the microbes present in the composting media were also involved in the degradation of the hydrogel polymer, leading to the cleavage of chemical bonds and bacterial degradation (Kaith, Jindal, Maiti, et al., 2010).

3.4.1. *Evidence of bio-degradation*

3.4.1.1. Spectroscopic studies. The FTIR spectrum of the Gg-cl-P(AAm-co-AN) hydrogel polymer was recorded at different stages of biodegradation (Fig. 4(a–d)). The FTIR of the Gg-cl-P(AAm-co-AN) hydrogel polymer before biodegradation exhibited peaks at 1673.25 cm^{-1} (C=O stretching of amide I band), 1453.57 cm^{-1} (NH in-plane bending of the amide II band), 1253.44 cm^{-1} (CN stretching vibrations of the amide III band), 749 cm^{-1} (OCN deformations of the amide IV band) and 2240.78 cm^{-1} (C≡N of acrylonitrile)

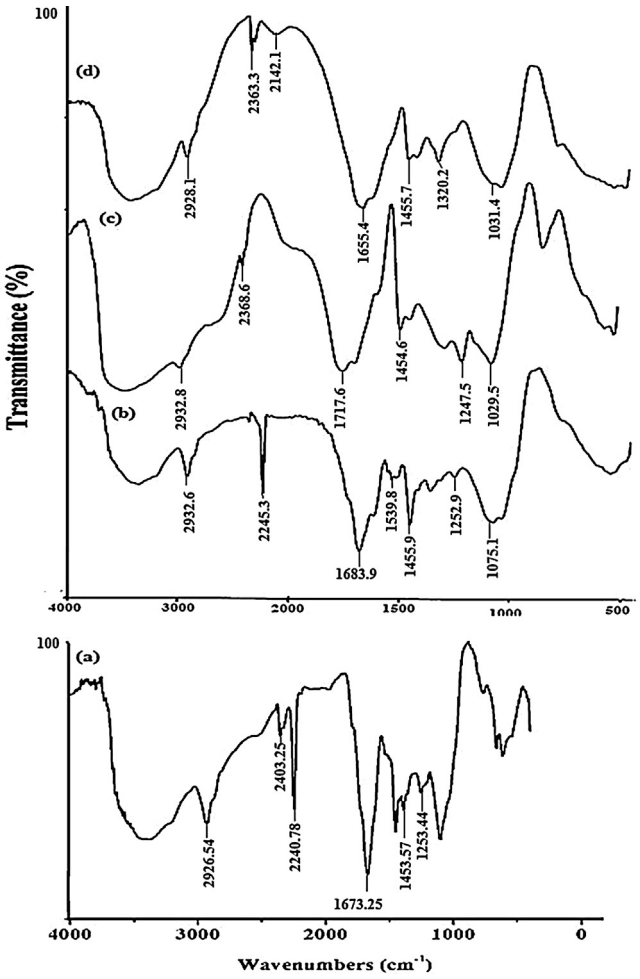

Fig. 4. FTIR spectra of (a) the Gg-cl-P(AAm-co-AN) hydrogel polymer, (b) the Gg-cl-P(AAm-co-AN) hydrogel polymer in stage I of biodegradation, (c) the Gg-cl-P(AAm-co-AN) hydrogel polymer in stage II of biodegradation, (d) the Gg-cl-P(AAm-co-AN) hydrogel polymer in stage III of biodegradation.

(Fig. 4(a)) in addition to the characteristic peaks of Gg (Kaith et al., 2012). However, the FTIR spectra of degraded samples at different stages of biodegradation showed peaks with reduced intensity and different peak positions compared to the FTIR spectrum of the Gg-cl-P(AAm-co-AN) hydrogel polymer before degradation. Peaks initially appearing at 1673.25 cm^{-1}, 2240.78 and 1453.57 cm^{-1} were shifted, with reduced intensity at biodegradation stage I (Fig. 4(b)). This may be due to the initiation of the breakdown of the cross-linked network. However, the degradation of individual compounds such as Gg and P(AAm-co-AN) began in the second stage of biodegradation (Fig. 4(c)). The major process in this stage was the degradation of Gg, together with the shifting or complete disappearance of the peaks related to the Gg. Most of the peaks initially appearing in the FTIR spectrum of the Gg-cl-P(AAm-co-AN) hydrogel polymer were completely shifted or absent in the third and final stage of biodegradation (Fig. 4(d)). Thus, FTIR studies at different stages of biodegradation confirmed that the grafted chains of P(AAm-co-AN) and Gg were biodegraded in the soil compost.

3.4.1.2. Morphology studies. The changes in the morphology of the Gg-cl-P(AAm-co-AN) hydrogel polymer at different stages of biodegradation were monitored using SEM (Fig. 5(a–d)). Before the degradation process started, the surface of the Gg-cl-P(AAm-co-AN) hydrogel polymer was found to be smooth and homogeneous, with a continuous and regular morphology (Fig. 5(a)). However, after the biodegradation process started, i.e., at the early stages of biodegradation (biodegradation stage-I), the number of cracks on the surface of the hydrogel polymer increased, and the homogeneous surface started becoming a fibrillar and heterogeneous surface (Fig. 5(b and c)). Some fractures and fissures also started to appear on the surface of the hydrogel polymer at the early stages of biodegradation, which confirmed the initiation of the degradation process. These fractures and fissures on the surface of the hydrogel polymer may be due to the initiation of the breakage of cross-links between different polymer chains, beginning the process of degrading individual components of the hydrogel polymer (Mittal, Mishra, et al., 2013). In the third and final stage of biodegradation, the size and number of these fissures and fractures were drastically increased, and the polymer surface became completely

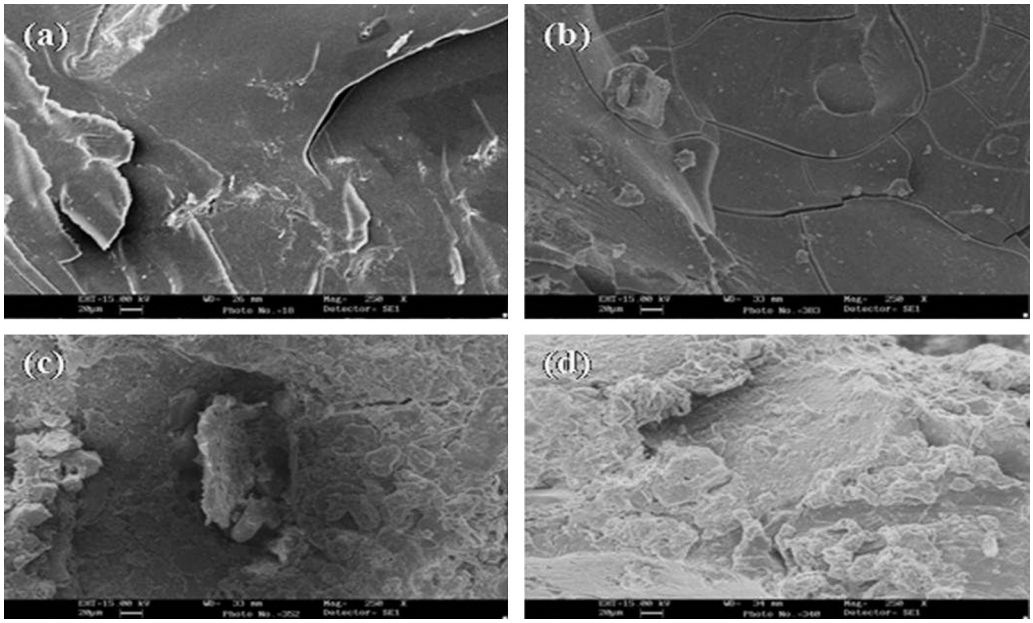

Fig. 5. SEM images of (a) the Gg-cl-P(AAm-co-AN) hydrogel polymer, (b) the Gg-cl-P(AAm-co-AN) hydrogel polymer in stage I of biodegradation, (c) the Gg-cl-P(AAm-co-AN) hydrogel polymer in stage II of biodegradation, (d) the Gg-cl-P(AAm-co-AN) hydrogel polymer in stage III of biodegradation.

Table 2
Percentage weight loss of Gg-cl-P(AAm-co-AN) hydrogel polymer using soil composting method.

Sample code	Percentage weight loss at different time intervals (days)											
	5	10	15	20	25	30	35	40	45	50	55	60
Gg-cl-P(AAm-co-AN)	11.53	16.25	21.95	33.96	37.50	41.86	48.93	57.62	65.37	73.05	77.14	89.47

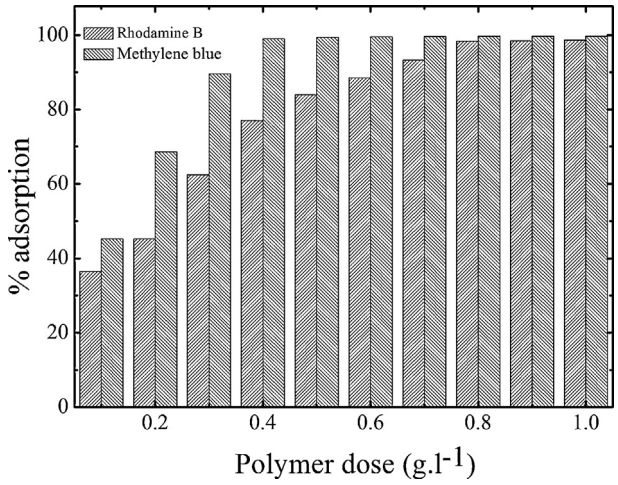

Fig. 6. Adsorption of methylene blue and rhodamine B using the Gg-cl-P(AAm-co-AN) hydrogel polymer.

rough and heterogeneous due to the complete fractured surface and the complete degradation of the individual components of the Gg-cl-P(AAm-co-AN) hydrogel polymer (Fig. 5(d)). This may be due to the complete breakage of covalent bonds between different polymeric chains through chemical and enzymatic degradation by the secreted products of different micro-organisms (Mittal, Mishra, et al., 2013). Thus, SEM studies predicted that enzymes secreted by micro-organisms were responsible for the degradation of the Gg-cl-P(AAm-co-AN) hydrogel polymer.

3.5. Adsorption of cationic dyes from the aqueous solution

The Gg-cl-P(AAm-co-AN) hydrogel polymer was successfully used for the adsorption of methylene blue and rhodamine B from aqueous solutions, and the results are shown in Fig. 6. The percentage adsorption was found to increase as the amount of hydrogel polymer increased. Almost 98% of methylene blue and rhodamine B were found to adsorb to 0.4 g l^{-1} and 0.8 g l^{-1} of the hydrogel polymer, respectively. We believe that the driving force for the high adsorption of cationic dyes using the Gg-cl-P(AAm-co-AN) hydrogel polymer is the electrostatic interaction between negatively charged functional groups of the hydrogel polymer and the cationic sites on the methylene blue and rhodamine B. As Gg is an anionic polysaccharide with abundant reactive hydroxyl and carboxylate ions (Aspinall et al., 1955; Aspinall, 1980), dye molecules can be easily attached to the binding sites of the Gg-cl-P(AAm-AN) hydrogel polymer.

4. Conclusions

A hydrogel-forming polymer of Gg with the co-polymer mixture of P(AAm-co-AN) was successfully synthesized and was found to be more thermally stable than Gg. The synthesized hydrogel polymer exhibited a maximum swelling capacity of 921% in neutral medium at 60 °C after 16 h. The Gg-cl-P(AAm-co-AN) hydrogel polymer also absorbed saline water from different saline water–petroleum fraction emulsions, and the maximum absorption of saline water was observed in the petroleum ether emulsion. Furthermore, the Gg-cl-P(AAm-co-AN) hydrogel polymer was found to exhibit very good flocculation characteristics, with the maximum flocculation efficiency observed with a 15 mg l^{-1} polymer dose in acidic medium at 40 °C. In soil composite, the Gg-cl-P(AAm-co-AN) hydrogel polymer was found to degrade 89.47% within 60 days, and changes in surface morphology and chemical composition were observed by SEM and FTIR. Moreover, The Gg-cl-P(AAm-AN) hydrogel polymer successfully removed more than 98% of cationic dyes from aqueous solution. This feasibility study confirmed that the hydrogel polymer synthesized here could be a good adsorbent for the removal of cationic dyes from industrial waste water.

Acknowledgments

The authors are grateful to the National Research Foundation, South Africa for awarding a postdoctoral research fellowship to Dr. Hemant Mittal. The authors (HM, AM, SSR) would also like to thank the Department of Science and Technology and the Council for Scientific and Industrial Research, South Africa for their financial support.

Appendix A. Supplementary data

Supplementary material related to this article can be found, in the online version, at http://dx.doi.org/10.1016/j.carbpol.2014.08.029.

References

Abrusci, C., Marquina, A. D. A., & Catalina, F. (2007). Biodegradation of cinematographic gelation emulsion by bacteria and filamentous fungi using indirect impedance technique. *International Biodeterioration and Biodegradation*, *60*, 137–143.
Aspinall, G. O. (1980). Chemistry of cell wall polysaccharides. In J. Preiss (Ed.), *The biochemistry of plants* (pp. 473–500). New York: Academic Press.
Aspinall, G. O., Hirst, E. L., & Wickstrom, A. (1955). Gum ghatti (Indian gum). The composition of the gum and the structure of two aldobiouronic acids derived from it. *Journal of the Chemical Society*, 1160–1165.
Averous, A., & Pollet, E. (2013). Macro-, micro-, and nanocomposites based on biodegradable polymers. In S. Thomas, D. Durand, C. Chassenieux, & P. Jyotishkumar (Eds.), *Handbook of biopolymers-based materials: From blends and composites to gels and complex networks* (pp. 173–210). Weinheim: Wiley-VCH Verleg GmbH & Co. KGaA.
Bajpai, S. K. (1999). Casein crosslinked polyacrylamide hydrogels: Study of swelling and drug release behaviour. *Iranian Polymer Journal*, *8*, 231–239.
Behari, K., Pandey, P. K., Kumar, R., & Taunk, K. (2001). Graft copolymerization of acrylamide onto Gum xanthan. *Carbohydrate Polymers*, *46*, 185–189.
Chang, Q., Hao, X., & Duan, L. (2008). Synthesis of crosslinked starch-graft-polyacrylamideco-sodium xanthate and its performance in waste water treatment. *Journal of Hazardous Materials*, *159*, 548–553.
Feil, H., Bae, Y. H., Feijen, J., & Kim, S. W. (1992). Mutual influence of pH and temperature on the swelling of ionizable and thermosensitive hydrogels. *Macromolecules*, *25*, 5528–5530.
Ghimici, L., & Constantin, M. (2011). Novel thermosensitive flocculating agent based on pullulan. *Journal of Hazardous Materials*, *192*, 1009–1016.
Ghimici, L., & Nichifor, M. (2010). Novel biodegradable flocculanting agents based on cationic amphiphilic polysaccharides. *Bioresource Technology*, *101*, 8549–8554.
Ghimici, L., & Nichifor, M. (2012). Flocculation by cationic amphiphilic polyelectrolyte: Relating efficiency with the association of polyelectrolyte in the initial solution. *Colloids and Surfaces A: Physicochemical and Engineering Aspects*, *415*, 142–147.
Ghimici, L., Dranca, I., Dragan, S., Lupascu, T., & Maftuleac, A. (2001). Hydrophobically modified cationic polyelectrolytes. *European Polymer Journal*, *37*, 227–231.
Ghimici, L., Constantin, M., & Fundueanu, G. (2010). Novel biodegradable flocculanting agents based on pullulan. *Journal of Hazardous Materials*, *181*, 351–358.

Ghimici, L., Constantin, M., & Fundueanu, G. (2012). Novel biodegradable flocculanting agents based on pullulan. *Journal of Hazardous Materials*, *181*, 351–358.
Ghorai, S., Sarkar, A., Raoufi, M., Panda, A. S., & Schonherr, H. (2014). Enhanced removal of methylene blue and methyl violet dyes from aqueous solution using a nanocomposite of hydrolysed polyacrylamide grafted xanthan gum and incorporated nanosilica. *ACS: Applied Materials Interface and Science*, *6*, 4766–4777.
Hermanova, S., Balkova, R., Voberkova, S., Chamradova, I., Omelkova, J., Richtera, L., et al. (2013). Biodegradation study on poly(ε-caprolactone) with bimodal molecular weight distribution. *Journal of Applied Polymer Science*, *127*, 4726–4735.
Inomato, H., Goto, S., & Saito, S. (1990). Phase transition of N-substituted acrylamide gels. *Macromolecules*, *23*, 4887–4888.
Jenkins, D. W., Samuel, M., & Hudson, S. M. (2001). Review of vinyl graft copolymerization featuring recent advances toward controlled radical-based reactions and illustrated with chitin/chitosan trunk polymers. *Chemical Review*, *101*, 3245–3274.
Jha, A., Agarwal, S., Mishra, A., & Rai, J. S. P. (2001). Synthesis, characterization and flocculation efficiency of poly(acrylamide-co-acrylic acid) in tanne. *Iranian Polymer Journal*, *10*, 85–90.
Kaith, B. S., Ranjta, S., & Kumar, K. (2008). In-air synthesis of GA-cl-poly(MAA) hydrogel and study of its salt-resistant swelling behavior in different salts. *e-Polymers*, *158*
Kaith, B. S., Jindal, R., Maiti, M., & Jana, A. K. (2010). Development of corn starch based green composites reinforced with *Saccharum spontaneum* L. fiber and graft copolymers—Evaluation of thermal, physico-chemical and mechanical properties. *Bioresource Technology*, *101*, 6843–6851.
Kaith, B. S., Jindal, R., & Mittal, H. (2010). Superabsorbent hydrogels from poly(acrylamide-co-acrylonitrile) grafted Gum ghatti with salt, pH and temperature responsive properties. *Der Chemica Sinica*, *1*, 92–103.
Kaith, B. S., Jindal, R., Mittal, H., & Kumar, K. (2012). Synthesis, characterization and swelling behavior evaluation of Gum ghatti and acrylamide based hydrogel for selective absorption of saline from different petroleum fraction—Saline emulsions. *Journal of Applied Polymer Science*, *124*, 2037–2047.
Kaur, I., Bhalla, T. C., Deepika, N., & Gautam, N. (2009). Study of the biodegradation behavior of soy protein-grafted polyethylene by the soil burial method. *Journal of Applied Polymer Science*, *111*, 2460–2467.
Kumari, K., & Abraham, T. E. (2007). Biosorption of anionic textile dyes by nonviable biomass of fungi and yeast. *Bioresource Technology*, *98*, 1704–1710.
Liang, Y., Xiao, L., Zhai, Y., Xie, C., Deng, L., & Dong, A. (2013). Preparation and characterization of biodegradable poly(sebacic anhydride) chain extended by glycol as drug carrier. *Journal of Applied Polymer Science*, *127*, 3948–3953.
Mahdavinia, G. R., Pourjavadi, A., Hosseizadeh, H., & Zohuriaan, M. J. (2004). Modified chitosan 4. Superabsorbent hydrogels from poly(acrylic acid-co-acrylamide) grafted chitosan with salt- and pH-responsiveness properties. *European Polymer Journal*, *40*, 1399–1407.
Mariano, M., El Kissi, N., & Dufresne, A. (2014). Cellulose nanocrystals and related nanocomposites: Review of some properties and challenges. *Journal of Polymer Science, Part B: Polymer Physics*, *52*, 791–806.
Mishra, M. M., Sand, A., Mishra, D. K., Yadav, M., & Behari, K. (2010). Free radical graft copolymerization of N-vinyl-2-pyrrolidone onto k-carrageenan in aqueous media and applications. *Carbohydrate Polymers*, *82*, 424–431.
Mittal, H., & Mishra, S. (2014). Gum ghatti and Fe_3O_4 magnetic nanoparticles based nanocomposites for the effective adsorption of Rhodamine B. *Carbohydrate Polymers*, *101*, 1255–1264.
Mittal, H., Fosso-Kankeu, E., Mishra, S., & Mishra, A. (2013). Biosorption potential of Gum ghatti-g-poly(acrylic acid) and susceptibility to biodegradation by *B. subtilis*. *International Journal of Biological Macromolecules*, *62*, 370–378.
Mittal, H., Mishra, S. B., Mishra, A. K., Kaith, B. S., & Jindal, R. (2013). Flocculation characteristics and biodegradation studies of Gum ghatti based hydrogels. *International Journal of Biological Macromolecules*, *58*, 37–46.
Mittal, H., Ballav, N., & Mishra, S. (2014). Gum ghatti and Fe_3O_4 magnetic nanoparticles based nanocomposites for the effective adsorption of methylene blue from aqueous solution. *Journal of Industrial and Engineering Chemistry*, *20*, 2184–2192.
Nageotte, V. M., Pester, C., Pradet, T. C., & Bayard, R. (2006). Aerobic and anaerobic biodegradation of polymer films and physic-chemical characterization. *Polymer Degradation and Stability*, *91*, 620–627.
Nasser, M. S., & James, A. E. (2006). The effect of polyacrylamide charge density and molecular weight on the flocculation and sedimentation behavior of kaolinite suspensions. *Separation and Purification Technology*, *52*, 241–252.
Okada, M. (2002). Chemical synthesis of biodegradable polymers. *Progress in Polymer Science*, *2002*, 87–133.
Pal, S., Sen, G., Karmakar, N. C., Mal, D., & Singh, R. P. (2008). High performance flocculating agents based on cationic polysaccharides in relation to coal fine suspension. *Carbohydrate Polymers*, *74*, 590–596.
Park, H., Park, K., & Kim, D. (2006). Preparation and swelling behavior of chitosan based superporous hydrogels for gastric retention application. *Journal of Biomedical Material Research Part A*, *76*, 144–150.
Sadeghi, S., Azhdari, H., Arabi, H., & Moghaddam, A. Z. (2012). Surface modified magnetic Fe_3O_4 nanoparticles as a selective sorbent for solid phase extraction of uranyl ions from water samples. *Journal of Hazardous Materials*, *215–216*, 208–216.
Sand, A., Yadav, M., & Behari, K. (2010). Graft co-polymeirzation of 2-acrylamidoglycolic acid onto xanthan gum and study of its physiochemical properties. *Carbohydrate Polymers*, *81*, 626–632.
Sand, A., Yadav, M., Mishra, M. M., Tripathy, J., & Behari, K. (2011). Studies on graft copolymerization of 2-acrylamidoglycolic acid on to partially carboxymethylated guar gum and physico-chemical properties. *Carbohydrate Polymers*, *83*, 14–21.
Sanghi, R., Bhattacharya, B., & Singh, V. (2006). Use of cassia javahikai seed gum and gum-g-polyacrylamide as coagulant aid for the decolorization of textile dye solutions. *Bioresource Technology*, *97*, 1259–1264.
Sarkar, A. K., Mandre, N. R., Panda, A. B., & Pal, S. (2013). Amylopectin grafted with poly (acrylic acid): Development and application of a high performance flocculant. *Carbohydrate Polymers*, *95*, 753–759.
Simon, S., Picton, L., Le Cerf, D., & Muller, G. (2005). Adsorption of amphiphilic polysaccharides onto polystyrene latex particles. *Polymer*, *46*, 3700–3707.
Singh, R. P., Tripathy, T., Karmakar, G. P., Rath, S. K., Karmakar, N. C., Pandey, S. R., et al. (2000). Novel biodegradable flocculants based on polysaccharides. *Current Science*, *78*, 798–803.
Thakur, V. K., Thakur, M. K., Raghavan, P., & Kessler, M. R. (2014). Progress in green polymer composites from lignin for multifunctional applications: A review. *ACS Sustainable Chemistry and Engineering*, *2*, 1072–1092.
Tian, D., & Xie, H. Q. (2008). Synthesis and flocculation characteristics of konjacglucomannan-g-polyacrylamide. *Polymer Bulletin*, *61*, 277–285.
Wan, X., Li, Y., Wang, X., Chen, S., & Gu, X. (2007). Synthesis of cationic guar gum-graft polyacrylamide at low temperature and its flocculating properties. *European Polymer Journal*, *43*, 3655–3661.
Xie, C., Feng, Y., Cao, W., Xia, Y., & Lu, Z. (2007). Novel biodegradable flocculating agents prepared by phosphate modification of konjac. *Carbohydrate Polymers*, *67*, 566–571.
Zare, E. N., Lakouraj, M. M., & Mohseni, M. (2014). Biodegradable polypyrrole/dextrin conductive nanocomposite: Synthesis, characterization, antioxidant and antibacterial activity. *Synthetic Metals*, *187*, 9–16.
Zhang, X. Z., Yang, Y. Y., Chung, T. S., & Ma, K. X. (2001). Preparation and characterization of fast response macroporous poly(N-isopropylacrylamide) hydrogels. *Langmuir*, *17*, 6094–6099.